

A Simulation Study on Continuous Direct Esterification Process for Poly(ethylene terephthalate) Synthesis

CHANG-KWON KANG,^{1*} BYOUNG CHUL LEE,¹ DAE WOO IHM,¹ and DAVID A. TREMBLAY²

¹R&D Center, Cheil Synthetics, Inc., SAIT, #14, Nongseo-Ri, Kiheung-Eub, Yongin-Gun, Kyonggi-Do, 449-900, Korea; ²Polymers Technology, Aspen Technology, Inc., Ten Canal Park, Cambridge, Massachusetts 02141

SYNOPSIS

A mathematical model for a continuous direct esterification reactor has been developed. The solid-liquid equilibrium of terephthalic acid (TPA) was considered in our modeling, and the characteristic dissolution time, an adjustable parameter, was introduced to account for the mass-transfer effect in the dissolution of TPA. The effects of the characteristic dissolution time, monomer feed ratio, temperature, and pressure on the reactor performance at different residence times were investigated through simulation. It was observed that the behavior of the first reactor strongly depends on whether the solid TPA is completely dissolved in the reaction mixtures. From the dynamic simulations, it was found that a sudden change in the operating conditions affects the ethylene glycol (EG) vapor flow rate instantly. For the esterification process having two reactors in series, the strategy for time distribution and recycling of EG is also discussed. © 1997 John Wiley & Sons, Inc.

INTRODUCTION

The continuous direct esterification of terephthalic acid (TPA) with ethylene glycol (EG) is one of the most popular manufacturing methods of poly(ethylene terephthalate) (PET), which is an important material for the production of synthetic fibers, films, and beverage bottles. During the esterification process, bis(hydroxyethyl)terephthalate and some linear oligomers are prepared, and water is evolved as a condensation byproduct.

Many simulation studies^{1,2} for the continuous direct esterification process have been made to develop a mathematical model for predicting the properties of the oligomers emerging from the reactors and the amount of byproducts such as diethylene glycol (DEG) from undesirable side reactions. Although these studies give useful information for the improvement of productivity and product quality, more elaborate efforts are required to obtain practical information for the optimization of the existing plants and the design of a new plant.

In this study, we developed a rigorous model for continuous direct esterification reactors, especially for the first reactor where the undissolved TPA may exist. The influence of the major operating conditions on reactor performance was investigated through model simulations, and particular attention was given to a correlation between the existing solid TPA and reactor performance. In dynamic tests, the responses of the first reactor to changes in operating conditions was examined. Additionally, specific strategy for designing an esterification process having two reactors in series is also discussed.

ASSUMPTIONS AND MODELING

Polymer Segment Approach

A modeling approach that properly accounts for varying chain lengths is required to establish a framework for representing polymer reaction kinetics. In this study, the polymer segment approach,³ a functional group approach, is used to establish the overall reaction network. Polymerization reactions can be regarded as reactions between two functional groups.

* To whom correspondence should be addressed.

All components considered in the reaction scheme are listed in Table I, where five different oligomeric segments are defined: tEG, tTPA, bEG, bTPA, and bDEG ("t" and "b" represent the "terminal functional group" and the "bound monomer repeating unit," respectively). Here, it should be noted that free TPA can be differentiated from the acidic oligomers (tTPA). This makes it more convenient to describe the solid-liquid equilibrium of TPA in the reaction mixtures than in the other functional group models used in the previous works.⁴

Using the polymer segment approach, the number-average degree of polymerization (DP) of the oligomers produced can be written as

$$DP = \frac{[tEG] + [bEG] + [tTPA] + [bTPA] + [bDEG]}{[tEG] + [tTPA]} \quad (1)$$

Reaction Scheme

The complete set of reactions considered here is shown in Table II. In this table, k_i ($i = 1-6$) are the "effective" rate constants (L/mol min) and K_i ($i = 1-5$) are the equilibrium constants. Reactions 1-4 are the esterification reactions, and reaction 5 is the polycondensation reaction.

It is known that DEG is formed in the esterification stage and in the beginning of the polycondensation stage, whereas acetaldehyde, acid end groups, and vinyl end groups are formed mainly in the final stages of polycondensation. Reaction 6 is a side reaction leading to the DEG formation. Al-

though several reaction mechanisms have been proposed to describe the DEG formation reaction, the mechanisms are lumped together in reaction 6.

Mathematical Model

Assuming that functional group reactivity does not depend on the polymer chain length, the material balance equation of each component in a continuous stirred tank reactor (CSTR) can be written as

$$V(dC_1^O/dt) = F^i C_1^i - F^O C_1^O + \rho V \{-R_1 - R_2 + R_5\} - F^V C_1^V + F^R C_1^R \quad (2)$$

$$V(dC_2^O/dt) = F^i C_2^i - F^O C_2^O + \rho V \{-R_1 - R_3\} \quad (3)$$

$$V(dC_3^O/dt) = F^i C_3^i - F^O C_3^O + \rho V \{R_1 + R_2 - R_3 - R_4 - 2R_5 - 2R_6\} \quad (4)$$

$$V(dC_4^O/dt) = F^i C_4^i - F^O C_4^O + \rho V \{R_1 - R_2 + R_3 - R_4\} \quad (5)$$

$$V(dC_5^O/dt) = F^i C_5^i - F^O C_5^O + \rho V \{R_3 + R_4 + R_5\} \quad (6)$$

$$V(dC_6^O/dt) = F^i C_6^i - F^O C_6^O + \rho V \{R_2 + R_4\} \quad (7)$$

$$V(dC_7^O/dt) = F^i C_7^i - F^O C_7^O + \rho V \{R_1 + R_2 + R_3 + R_4 + R_6\} - F^V C_7^V + F^R C_7^R \quad (8)$$

$$V(dC_8^O/dt) = F^i C_8^i - F^O C_8^O + \rho V R_6 \quad (9)$$

Table I Molecular Structures of Components Considered


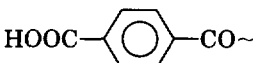
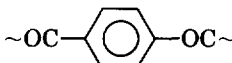
Symbol	Descriptions	Molecular Structure
TPA	Terephthalic acid	
EG	Ethylene glycol	HOCH ₂ CH ₂ OH
W	Water	H ₂ O
tEG	EG end group	HOCH ₂ CH ₂ O~
tTPA	TPA end group	
bEG	EG repeat unit	~OCH ₂ CH ₂ O~
bTPA	TPA repeat unit	
bDEG	Diethylene glycol repeat unit	~OCH ₂ CH ₂ OCH ₂ CH ₂ O~

Table II Reaction Scheme of Esterification Process Considered in This Work

No.	Reactions	Rate Constants	
		Forward,	Reverse
(1)	$\text{EG} + \text{TPA} \rightleftharpoons \text{tEG} + \text{tTPA} + \text{W}$	$k_1,$	k_1/K_1
(2)	$\text{EG} + \text{tTPA} \rightleftharpoons \text{tEG} + \text{bTPA} + \text{W}$	$k_2,$	k_2/K_2
(3)	$\text{tEG} + \text{TPA} \rightleftharpoons \text{bEG} + \text{tTPA} + \text{W}$	$k_3,$	k_3/K_3
(4)	$\text{tEG} + \text{tTPA} \rightleftharpoons \text{bEG} + \text{bTPA} + \text{W}$	$k_4,$	k_4/K_4
(5)	$\text{tEG} + \text{tEG} \rightleftharpoons \text{bEG} + \text{EG}$	$k_5,$	k_5/K_5
(6)	$\text{tEG} + \text{tEG} \rightarrow \text{bDEG} + \text{W}$	k_6	

where F^i and F^o represent the input and output flow rates, respectively; V , the liquid phase volume free from the undissolved TPA; and ρ , the density of the reaction melt. F^V and F^R are the vapor flow rate to the distillation column attached and the reflux flow rate from the column, respectively. For the constant reactor volume, the following relation holds:

$$F^i + F^R = F^o + F^V \quad (10)$$

C_j^i ($j = 1-8$) and C_j^o ($j = 1-8$) represent the input and output concentrations, respectively, of the components in the reaction mixture containing the undissolved TPA. Here, the numbers 1-8 denote EG, TPA, tEG, tTPA, bEG, bTPA, W, and bDEG, respectively. In eq. (3), C_2^o is the total amount of TPA in the output flow, i.e., $C_2^o = C_L^o + C_S^o$, where C_L^o and C_S^o are the output concentrations of the liquid TPA and undissolved solid TPA, respectively. C_1^V and C_7^V and C_1^R and C_7^R are the concentrations of EG and W in the vapor flow and in the reflux flow, respectively.

R_i ($i = 1-6$) are the reaction rates for reactions 1-6, and they can be written as

$$R_1 = 4k_1C_1C_2 - (k_1/K_1)C_4C_7 \quad (11)$$

$$R_2 = 2k_2C_1C_4 - 2(k_2/K_2)C_6C_7 \quad (12)$$

$$R_3 = 2k_3C_3C_2 - (k_3/K_3)C_4C_7 \quad (13)$$

$$R_4 = k_4C_3C_4 - 2(k_4/K_4)C_6C_7 \quad (14)$$

$$R_5 = k_5C_3C_3 - 4(K_5/K_5)C_1C_5 \quad (15)$$

$$R_6 = k_6C_3C_3 \quad (16)$$

Here, C_j represents the concentration of component j in the liquid phase of the reaction mixture free from the undissolved TPA, and it can be written as

$$C_j = C_j^o \frac{F^o}{F^o - F^S} \quad (\text{for } j = 1, 3-8) \quad (17-1)$$

$$C_2 = C_L^o \frac{F^o}{F^o - F^S} \quad (\text{for } j = 2) \quad (17-2)$$

where F^S is the flow rate of undissolved solid TPA.

Phase Equilibrium

For the calculation of the concentrations of volatile components (EG and water) in the liquid and in the vapor phases, a quasi-steady-state assumption is used for the vapor-liquid equilibrium. No vapor-phase calculations of the oligomeric components are considered since the polymer is not volatile.

The vapor phase is assumed to follow the ideal gas law:

$$p_j = p_T \cdot y_j \quad (18)$$

where p_T is the total pressure of the reactor, and p_j and y_j , the partial pressure and mol fraction of volatile component j in the vapor phase. Using Raoult's law, the partial pressure of volatile components will be given by

$$p_j = p_j^* \cdot x_j \quad (19)$$

where p_j^* is the saturated vapor pressure of volatile component j , and x_j , the mol fraction of component j in the liquid phase. The vapor pressure data of water and EG are obtained from a pure component databank.⁵

Since the solubility of TPA in EG is extremely low and the esterification is occurring in the liquid phase, the solid-liquid equilibrium of TPA should be considered to calculate the concentration of each component in the liquid phase (C_1-C_8). Assuming that the solubility of TPA in water is negligible, the

Table III Numerical Values Used for the Calculation

Reaction No.	Preexponent Factor (A_i)	Activation Energy (E_i)	Equilibrium Constant (K_i)
1, 2	4.68×10^5 (L/mol) ² /min	18.0 kcal/mol	2.50
3, 4	2.34×10^5 (L/mol) ² /min	18.0 kcal/mol	1.25
5	3.64×10^5 (L/mol) ² /min	18.0 kcal/mol	0.50
6	2.17×10^9 (L/mol)/min	29.8 kcal/mol	—

(2) Temperature dependencies of solubility of TPA in EG and in BHET

$$\alpha_{EG} = 9062 \exp(-4877/T) \text{ (TPA mol in 1 kg EG)}$$

$$\alpha_{BHET} = 374 \exp(-3831/T) \text{ (TPA mol in 1 kg BHET)}$$

(T is the absolute temperature)

(3) Vapor pressures of EG and water

$$\text{For EG, } \ln p = 79.3 + (-10105/T) + (-7.5 \times \ln T) + 7.3e^{-19} \times T^6$$

$$\text{For W, } \ln p = 73.6 + (-7259/T) + (-7.3 \times \ln T) + 4.2e^{-6} \times T^2$$

(p is vapor pressure in Pa)

(4) Density of the reaction melt

$$\rho = 1.110 \text{ (kg/L)}$$

mean solubility of TPA (α) in the reaction mixtures can be given by⁶

$$\alpha = \alpha_{EG} W_{EG} + \alpha_{BHET} W_{OLG} \quad (20)$$

where α_{EG} and α_{BHET} are the solubility of TPA in EG and BHET, respectively, and W_{EG} and W_{OLG} are the weight fractions of EG and of oligomers, respectively. The experimental data by Yamada et al.⁶ were used for the calculation of α_{EG} and α_{BHET} .

Acid-catalyzed Reactions

For solving the material balance equations, one must estimate the rate constants k_i ($i = 1-6$) and the equilibrium constants K_i ($i = 1-5$). From previous works,^{1,2} it can be assumed that the reactivity of the acid end group on TPA is equivalent to the reactivity on an oligomer chain (tTPA) while the reactivity of the hydroxyl end group on EG is different from the reactivity on half-esterified EG (tEG), i.e., $k_1 = k_2$ and $k_3 = k_4$. In reverse esterifications, water attacks an ester link, splitting the polymer molecule into two smaller molecules. Similarly, it can be assumed that $(k_1/K_1) = (k_2/K_2)$ and $(k_3/K_3) = (k_4/K_4)$.

The rate constants are dependent on temperature, catalyst type, and catalyst concentration. According to previous works,^{6,7} it can be assumed that the rate

constants for the acid-catalyzed esterification and polycondensation are written as

$$k_i = A_i C_{acid} \exp(-E_i/RT) \quad (\text{for } i = 1-5) \quad (21)$$

where A_i is the preexponent factor (L²/mol² min); E_i , the activation energy; R , the gas constant; T , the temperature in K; and C_{acid} , the total acid concentration. In this study, C_{acid} can be defined as

$$C_{acid} = 2C_2 + C_4 \quad (22)$$

where C_2 and C_4 are the concentrations of the dissolved TPA and tTPA in the liquid phase of the reaction mixture free from the undissolved TPA, respectively.

For the values of the equilibrium constants, K_1 ($= K_2$), K_3 ($= K_4$), and K_5 , and of the rate constants, k_1 ($= k_2$), k_3 ($= k_4$), and k_5 , the results of an experimental work by Otton and Ratton⁸ were used in this study. (see Table III). No experimental result for the rate constant for the DEG formation has been published. For the estimation of k_6 , we used the kinetic parameters used in a simulation study of Ravindranath and Mashelkar.⁹

Numerical Computation Procedure

As indicated in Table II, reactions 1–4 are reversible. In industrial practice, the condensation byproduct, water, is distilled off continuously from the reactor to promote the forward reactions. In this study, it is assumed that all vaporized EG is refluxed and all vaporized water is removed from the distillation column, i.e., $F^V C_1^V = F^R C_1^R$ and $F^V C_7^V = 0$. This perfect separation simplifies the flash calculation and causes negligible errors.

For the steady-state simulation, the differential equations of the material balance equations [eqs. (2)–(9)] are directly converted into the corresponding nonlinear algebraic ones with the left-hand side set to zero, which are solved by the following procedure:

Step #1: Make an initial guess for F^V .

Step #2: (1) Make initial guesses for C_1^O to C_8^O ; (2) calculate C_L^O , C_S^O , and F^S by using eq. (20); (3) calculate C_1 to C_8 by using eq. (17); (4) calculate C_1^V and C_7^V by using eqs. (18) and (19); (5) determine $F^{O'}$ by using eq. (10); and (6) solve eqs. (2)–(9) by using the multivariable Newton–Raphson method.

Step #3: (1) Calculate p_T by using eq. (18); (2) if the difference between the calculated pressure and the system pressure is less than a tolerance, the calculation stops; (3) if not so, the calculation returns to Step #1 to make a new guess for F^V .

For the dynamic-state simulation, the differential governing eqs. (2)–(9) are solved simultaneously by using the fourth-order Runge–Kutta method. The initial conditions for all the state variables are obtained by solving the steady-state modeling equations.

RESULTS AND DISCUSSION

It would have been desirable to validate the above model equations with plant or pilot plant data. A pilot plant study of Yamada et al.¹⁰ is the only source in the open literature concerning the direct continuous esterification process. However, their data cannot be quantitatively compared with our modeling results, since they used a higher monomer feed ratio ($[EG]_0/[TPA]_0 = 2.0$) and lower pressures (1.0 and 2.0 atm) which are somewhat different from the operating conditions considered here. Some proprietary industrial data available to us indicate

a reasonable agreement in a semiquantitative way. The results from this simulation study may be helpful to understand the continuous direct esterification process, although rigorous comparisons with plant data cannot be presented.

Steady-state Analysis of the First Esterification Reactor

One of the main objectives in operating esterification reactors is to achieve a high conversion of TPA in a short reactor residence time. In this section, we examine the effects of various operating conditions on the performance of the first esterification reactor. For model simulations, operating conditions very close to real practice are used.

In the direct esterification process, the extremely low solubility of TPA in EG might bring in a mass-transfer limitation due to the slow rate of TPA dissolution. In trying to examine the mass-transfer effect of solid TPA, we assumed that the apparent solubility (α') can be written by the following simple equation:

$$\alpha' = \frac{\alpha}{1 + (\tau/\theta)} \quad (23)$$

where θ is the residence time, and τ , the characteristic dissolution time which is a function of the shape and size of the solid TPA particles and the mixing characteristics of the reactor. Although the validity of eq. (23) has not been proved, the newly introduced parameter, τ , may be available to simplify the model simulation.

Figure 1 shows the effects of τ on the conversion of acid end groups and the concentration of the undissolved solid TPA in the oligomers produced at three different residence times. As expected, it is shown that as τ is increased the conversion decreases and the solid TPA increases. It is interesting to note that there is a small region not affected by the variation in τ in the 300 min case. This reason is that the solubility of TPA has no effect on the reactions at high conversions where all the solid TPA molecules are dissolved and consumed for the reactions. Hence, it is inferred that one should increase the residence time to reduce the mass-transfer effect of the solid TPA on the reactions.

The monomer feed ratio is one of the most important operating variables in the esterification process. Generally, more EG is available to increase the solubility of TPA and to increase the conversion of the reactions. However, the use of more EG is not economical in terms of the large energy require-

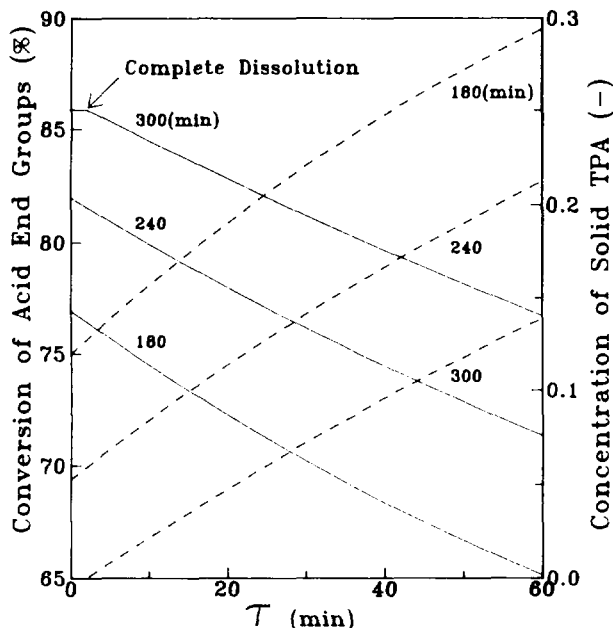


Figure 1 Effects of characteristic dissolution time of TPA (τ) on the conversion and concentration of the undissolved solid TPA in the oligomers produced at the indicated residence times. τ is defined as eq. (23). The solid and dotted lines are the conversions and solid concentrations, respectively. The concentrations are nondimensionalized with respect to $[\text{TPA}]_0$. For the calculations, it is assumed that the monomer feed ratio is 1.20, temperature 260°C , and pressure 2.0 atm.

ment of EG vaporization and condensation. Therefore, this is a good reason to determine the optimum ratio through simulations.

Figure 2 shows the effect of the monomer feed ratio on the conversion for three different cases. In this figure, it is shown that more EG is required to dissolve all the solid TPA at the longer dissolution time ($\tau = 20$ min). Also, one can easily find that as the ratio is increased the conversion increases. However, the slope of the curve is reduced after the complete dissolution of solid TPA is reached, because the dissolved TPA molecules promote the forward reactions of the esterification. Moreover, they act as an acidic catalyst for the reactions.

Figure 3 shows the effect of the monomer feed ratio on the EG vapor flow rate at various residence times. In this figure, after the complete dissolution of solid TPA, the EG vapor flow rate is sharply increased with increasing the ratio. This indicates that the excess EG over the complete dissolution of solid TPA wastes energy, although more EG is useful to increase the conversion.

When the monomer feed ratio is kept constant, the reaction temperature can also influence the re-

action rate. Figure 4 shows the results concerning the effect of the reaction temperature on the conversion and EG vapor flow rate at various residence times. As expected, it is found that the conversion is increased with increasing temperature. The EG vapor flow rate is usually decreased at high temperatures, since more EG is consumed by the reactions. However, one can find that the EG vapor flow rate is slightly increased with increasing temperature after the complete dissolution of solid TPA. This implies that the increment in the EG vapor pressure is greater than the consumption of EG at high temperatures.

Generally, the first esterification reactor is operated under pressurized conditions. Figure 5 shows the effect of pressure on the conversion and EG vapor flow rate at three different residence times. In this figure, it is found that for the shorter residence times (180 and 240 min) the conversion increases as pressure is increased, because the solubility of TPA in the reaction mixture is increased for high pressures, due to the increment in the EG concentration in the liquid phase. Therefore, increasing the reactor pressure may have the advantage of reducing

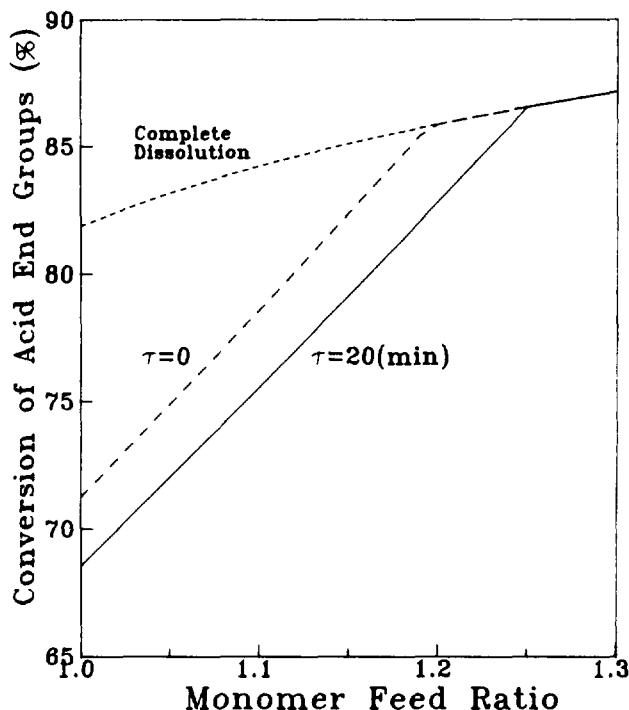


Figure 2 Effect of monomer feed ratio on the conversion. The dotted line is calculated for the assumption that the solid TPA is completely dissolved. The solid and broken lines are for $\tau = 0$ and $\tau = 20$ (min), respectively. For the calculations, it is assumed that temperature is 260°C and pressure 2.0 atm.

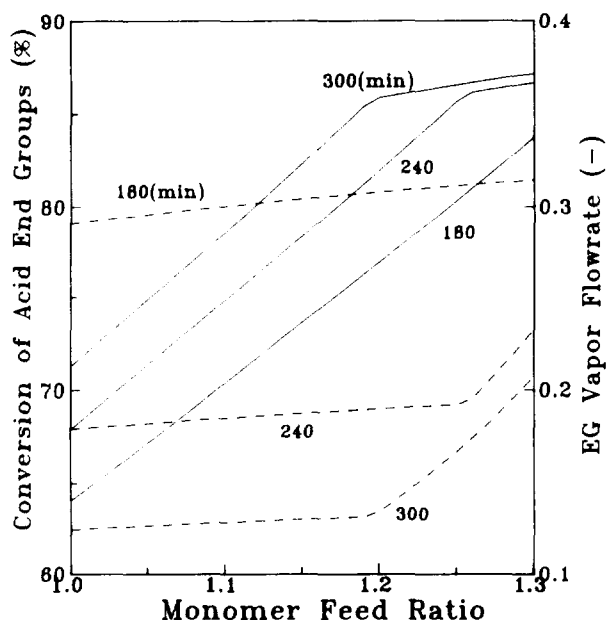


Figure 3 Effects of monomer feed ratio on the conversion and EG vapor flow rate. The solid and dotted lines are the conversions and flow rates at the indicated residence times, respectively. The flow rates are nondimensionalized with respect to the feed flow rate. For the calculations, it is assumed that τ is zero, temperature 260°C, and pressure 2.0 atm.

the EG vapor and increasing the conversion at shorter residence times. However, after the solid TPA is completely dissolved, the conversion is decreased with increasing pressure, as seen in the curve for the 300 min case. This is due to the consideration of the chemical and phase equilibrium. Thus, it is implied that one can determine whether the oligomers emerging from the reactor contain the undissolved solid TPA or not by analyzing the effect of pressure on the conversion.

Transient Behaviors of the First Esterification Reactor

In terms of process control, it is necessary to understand the transient reactor behaviors for several types of perturbation. In this section, the transient responses of the first esterification reactor are examined by making step changes in operating variables.

Trouble in the agitator may cause a sudden change in the mixing characteristics during the operation. When the characteristic dissolution time, τ , is increased, the solubility of TPA in the reaction mixture and the concentration of liquid TPA may decrease. In Figure 6, after a change in τ from 0 to

20 min, the conversion decreases to reach a new steady state. Since the sudden decrease in the concentration of the liquid TPA indicates a big drop in the rate of the esterification reactions, the EG mol fraction in the liquid phase is abruptly increased just after the perturbation. More EG should be vaporized to retain vapor-liquid equilibrium, and this generates an overshoot in the EG vapor flow rate as shown in the figure. Also, the sudden increase in the EG mol fraction means a sharp decrease in the water mol fraction in the liquid phase, and this causes a drop in the water vapor flow rate. This kind of dramatic change in the vapor flow rate may cause clogging problems in the distillation column.

Figure 7 shows the responses to a step change in the monomer feed ratio ($[EG]_0/[TPA]_0$) from 1.20 to 1.15. In the figure, after the perturbation, the conversion is decreased with time. The small decrease in the concentration of liquid TPA arises from a slight decrease in the solubility of TPA in the reaction mixtures with less EG, while the increasing concentration of solid TPA is due to the decrease in the rate of TPA consumption reactions. A sudden decrease in the EG mol fraction in the liquid phase causes a sharp decrease in the EG vapor flow rate.

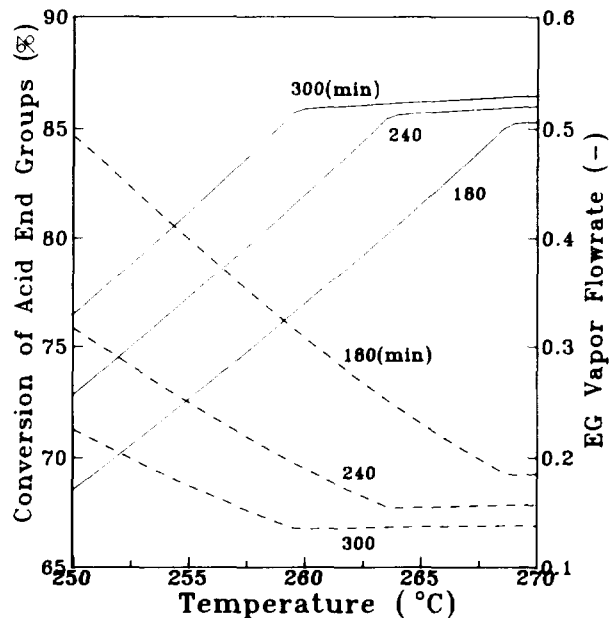


Figure 4 Effects of reaction temperature on the conversion and EG vapor flow rate. The solid and dotted lines are the conversions and flow rates at the indicated residence times, respectively. The flow rates are nondimensionalized with respect to the feed flow rate. For the calculations, it is assumed that τ is zero, monomer feed ratio 1.20, and pressure 2.0 atm.

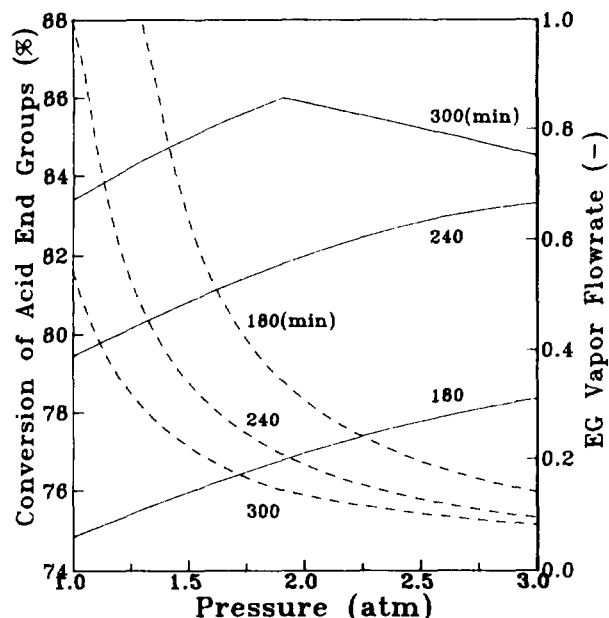


Figure 5 Effects of pressure on the conversion and EG vapor flow rate. The solid and dotted lines are the conversions and flow rates at the indicated residence times, respectively. The flow rates are nondimensionalized with respect to the feed flow rate. For the calculations, it is assumed that τ is zero, monomer feed ratio 1.20, and temperature 260°C.

When the residence time is decreased, the conversion decreases and the solid TPA increases as seen in Figure 8. However, the change in residence time does not greatly affect the solubility of TPA and the concentration of dissolved TPA. In the figure, the responses of the vapor flow rates to a step change in residence time are very similar to the τ -increase case above.

When the reaction temperature is decreased, the reaction rate and solubility of TPA decrease. This causes a decrease in the conversion as shown in Figure 9. In this figure, just as the τ -increase case, the overshoot in the EG vapor flow rate is arises from the sudden increase in the EG mol fraction in the liquid phase, although the lower temperature reduces the vapor flow rate. In real practice, however, it is difficult to make that kind of a sharp change in temperature due to the poor thermal conductivity of the reaction mixtures.

The response to a step decrease in the reactor pressure is shown in Figure 10. In this figure, one can notice that after the perturbation the conversion slightly increases and then decreases to reach a new steady state. This temporary increase in the conversion may be explained by the fact that the removal of water vapor promotes the reactions con-

suming the acidic oligomers (tTPA). Generally, the vapor flow rates are increased at low pressures but the water vapor flow rate is slightly decreased, as shown in the figure. This reason is that the decrease in the water mol fraction in the liquid phase compensates the increase in the vapor flow at low pressures.

From the above dynamic tests, it is found that this type of perturbation may generate a huge overshoot or undershoot in the EG vapor flow rate, causing a serious problem in operating the attached distillation column. Therefore, in trying to control the reactor safely, one should minimize the amount of EG vapor by promoting the EG consumption reactions. In comparison with the transesterification process which is another route for the synthesis of PET,^{11,12} it takes a much longer time for the system to reach to the new steady state for the step changes in the direct esterification process.

Two CSTRs in Series

In industrial practice, two or more reactors are usually used in series for the direct esterification stage to obtain a high conversion of TPA. From

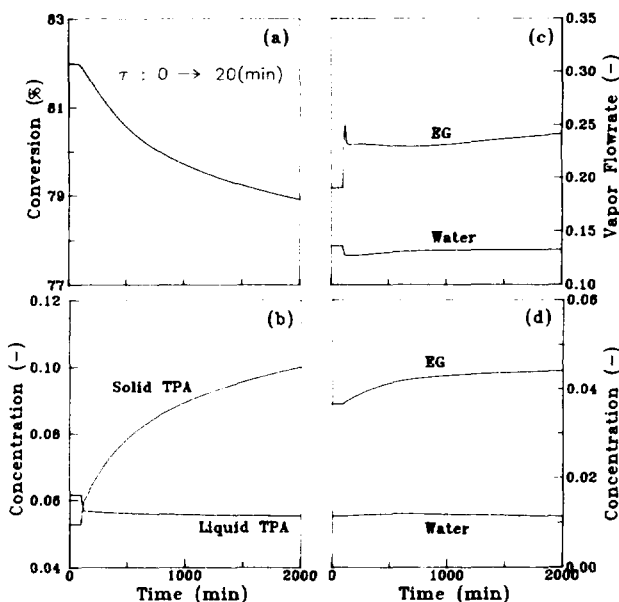


Figure 6 Transient responses to step change in τ from 0 to 20 min: (a) conversion of acid end groups; (b) concentrations of the solid and liquid TPA in the oligomers produced; (c) vapor flow rates of EG and water; (d) liquid concentrations of EG and water. The concentrations are nondimensionalized with respect to $[TPA]_0$. For the calculation, it is assumed that residence time is 240 min, monomer feed ratio 1.20, temperature 260°C, and pressure 2.0 atm.

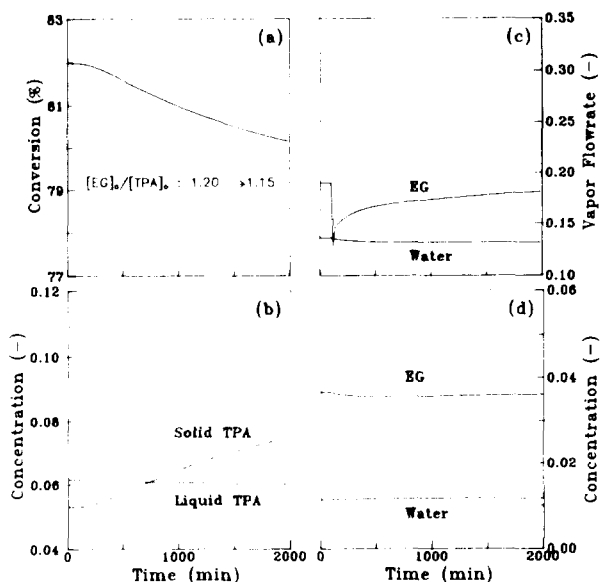


Figure 7 Transient responses to step change in monomer feed ratio from 1.20 to 1.15: (a) conversion of acid end groups; (b) concentrations of the solid and liquid TPA in the oligomers produced; (c) vapor flow rates of EG and water; (d) liquid concentrations of EG and water. The concentrations are nondimensionalized with respect to $[TPA]_0$. For the calculation, it is assumed that τ is zero, residence time 240 min, temperature 260°C, and pressure 2.0 atm.

the previous simulation study,¹ it was shown that a specific strategy of time and temperature distribution is required for an increase in TPA conversion and a reduction in the formation of side products. In this section, we examine the steady-state behavior of two CSTRs in series and suggest a specific strategy for time distribution and recycling of EG.

Here, the two reactors are assumed to have separate distillation columns and they are operated under different temperatures and pressures from each other: 260°C, 2 atm for the first CSTR, and 265°C, 1 atm for the second one, respectively. The monomer feed ratio is assumed to be 1.20. In real practice, a metal catalyst such as antimony oxide is usually fed to the second CSTR and promotes the reactions. For simplicity, however, the effect of the metal catalyst is not considered here.

At first, to examine the time distribution strategy for the two CSTRs, we set the total residence time for the two reactors at 400 min based on the feed flow rate of the first CSTR and then observed the reactor performance in variation of the residence time of the first CSTR. In Figure 11, the conversions

of the two CSTRs and EG vapor flow rate from the first CSTR are plotted against the residence time of the first CSTR at the fixed total residence time of 400 min. It is seen that the maximum conversion is achieved at the point where the solid TPA is completely dissolved in the first CSTR. As shown in the figure, the oligomers produced at the maximum conversion point have also the minimum value of DEG with an acceptable *DP*.

As described earlier, the residence time of the first CSTR should be long enough to dissolve more solid TPA molecules in order to increase the conversion of the reactions. However, increasing residence time has many limitations. Then, instead of increasing residence time, the recycle of the EG condensed at the second distillation column to the first CSTR may be suggested to increase the conversion in the first CSTR. In Figure 12, the conversions of the two CSTRs are plotted against the ratio of the recycled EG to the first CSTR to the total EG vapor from the second one. In this figure, it is observed that as the ratio is increased the conversions increase and the solid TPA decreases. The recycling EG to the first CSTR has no large effects on the DEG formation and the *DP* of oligomers, as shown in the figure.

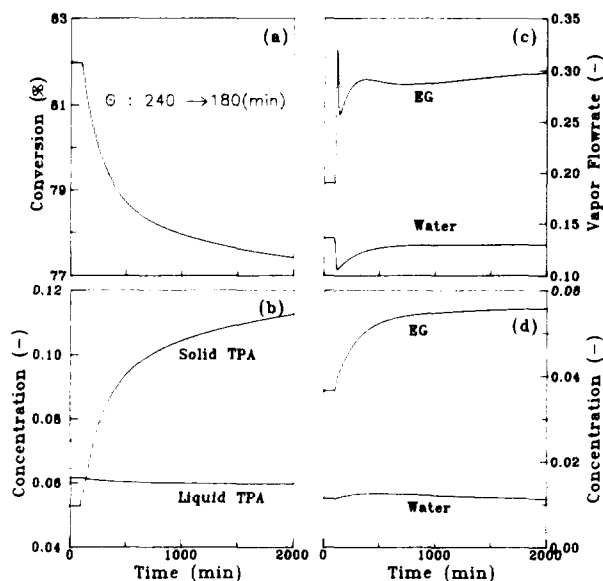


Figure 8 Transient responses to step change in residence time from 240 to 180 min: (a) conversion of acid end groups; (b) concentrations of the solid and liquid TPA in the oligomers produced; (c) vapor flow rates of EG and water; (d) liquid concentrations of EG and water. The concentrations are nondimensionalized with respect to $[TPA]_0$. For the calculation, it is assumed that τ is zero, monomer feed ratio 1.20, temperature 260°C, and pressure 2.0 atm.

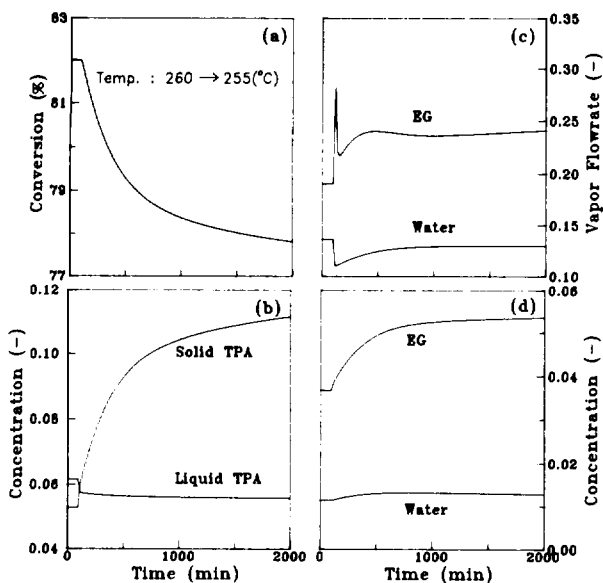


Figure 9 Transient responses to step change in reaction temperature from 260 to 255°C: (a) conversion of acid end groups; (b) concentrations of the solid and liquid TPA in the oligomers produced; (c) vapor flow rates of EG and water; (d) liquid concentrations of EG and water. The concentrations are nondimensionalized with respect to $[TPA]_0$. For the calculation, it is assumed that τ is zero, residence time 240 min, monomer feed ratio 1.20, and pressure 2.0 atm.

CONCLUSIONS

We have developed a mathematical model to carry out steady and dynamic simulations for continuous direct esterification reactors. The solid-liquid equilibrium of TPA was considered in our modeling, and the characteristic dissolution time was newly introduced to estimate the apparent solubility of TPA.

The influence of various operating conditions on the performance of the first esterification reactor was investigated through model simulations. It was observed that the reactor behavior strongly depends on whether the solid TPA is completely dissolved or not in the reaction mixtures.

The dynamic testing indicated that a sudden change in the operating conditions affects the EG vapor flow rate instantly and suggested that the amount of EG vapor should be reduced to control the reactor by promoting the EG consumption reactions. This work is the first to show the dynamic behavior of the continuous direct esterification reactor.

For the two CSTRs in series, it was found that the maximum conversion is achieved at the point where the solid TPA is completely dissolved in the

first CSTR. It was also shown that it is useful to increase the conversion by recycling the EG condensed at the second distillation column to the first CSTR.

We have undertaken simulations in a range that is as close to industrial practice as possible, but we could not validate the model equations against the plant data. However, it is hoped that the results of this simulation study would give useful information for the design of esterification reactors.

NOTATION

- A_i preexponent factor in rate expression of reaction i ($i = 1-6$)
 C_{acid} total acid concentration (mol/L), defined as eq. (22)
 C_j concentration of component j in liquid phase of reaction mixtures free from undissolved TPA (mol/L)
 C_j^i inlet concentration of component j in reaction mixture containing undissolved TPA (mol/L)

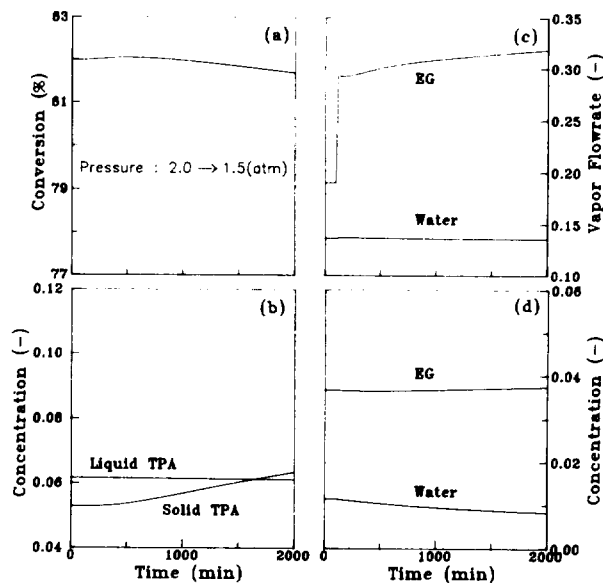


Figure 10 Transient responses to step change in pressure from 2.0 to 1.5 atm: (a) conversion of acid end groups; (b) concentrations of the solid and liquid TPA in the oligomers produced; (c) vapor flow rates of EG and water; (d) liquid concentrations of EG and water. The concentrations are nondimensionalized with respect to $[TPA]_0$. For the calculation, it is assumed that τ is zero, residence time 240 min, monomer feed ratio 1.20, and temperature 260°C.

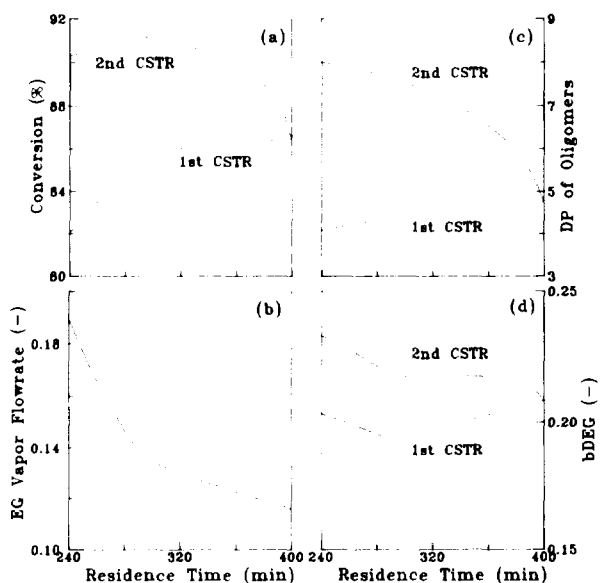


Figure 11 Effects of time distribution for two CSTRs in series: (a) conversion of acid end groups, (b) EG vapor flow rate in the first CSTR; (c) DP of the oligomers produced; (d) concentration of bDEG. The X-axis is the residence time of the first CSTR, and the total residence time for the two reactors is fixed to 400 min. The flow rate is nondimensionalized with respect to the feed flow rate. For the calculation, it is assumed that τ is zero, and monomer feed ratio, 1.20. The temperatures and pressures of the first and second CSTRs are 260°C, 2.0 atm and 265°C, 1.0 atm, respectively.

C_j^O	outlet concentration of component j in reaction mixture containing undissolved TPA (mol/L)
C_L^O	outlet concentration of dissolved TPA (mol/L)
C_S^O	outlet concentration of undissolved TPA (mol/L)
C_j^R	concentration of volatile component j in reflux flow (mol/L)
C_j^V	concentration of volatile component j in vapor flow (mol/L)
DP	number-average degree of polymerization for oligomers
F_i	activation energy for reaction i ($i = 1-6$)
F^i	feed flow rate to reactor (kg/h)
F^O	outlet flow rate of reaction mixture containing undissolved TPA (kg/h)
F^R	reflux flow rate from distillation column (kg/h)
F^S	outlet flow rate of undissolved TPA (kg/h)
F^V	vapor flow rate to distillation column (kg/h)

j	component, 1 to 8 represent EG, TPA, tEG, tTPA, bEG, bTPA, W, and bDEG, respectively
k_i	effective rate constant (L/mol min) for reaction i ($i = 1-6$)
K_i	equilibrium constant for reaction i ($i = 1-5$)
p_j	partial pressure of volatile component j in vapor phase
p_j^*	saturated vapor pressure of volatile component j
p_T	total pressure (reaction pressure)
R	gas constant
R_i	reaction rate for reaction i ($i = 1-6$)
T	reaction temperature
V	liquid phase volume of reaction mixtures in a reactor free from undissolved TPA (L)
W_{EG}	weight fraction of EG in reaction mixtures
W_{OLG}	weight fraction of oligomers in reaction mixtures
x_j	mol fraction of component j in liquid phase

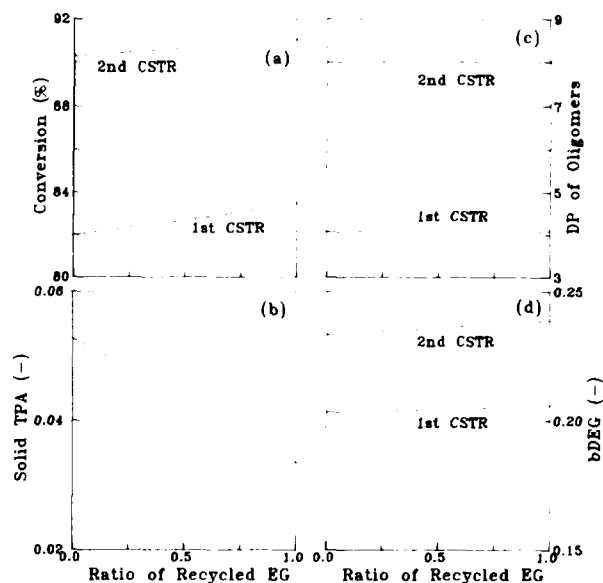


Figure 12 Effects of recycling EG from the second CSTR to the first one: (a) conversion of acid end groups; (b) concentration of undissolved solid TPA in the first CSTR; (c) DP of the oligomers produced; (d) concentration of bDEG. The concentration is nondimensionalized with respect to $[TPA]_0$. For the calculation, it is assumed that τ is zero and monomer feed ratio 1.20. The residence times, temperatures, and pressures of the first and second CSTRs are 240 min, 260°C, 2.0 atm and 160 min, 265°C, 1.0 atm, respectively.

y_j	mol fraction of volatile component j in vapor phase
$[EG]_0$	concentration of EG in feed (mol/L)
$[TPA]_0$	concentration of TPA in feed (mol/L)
α_{BHET}	solubility of TPA in BHET (mol/kg)
α_{EG}	solubility of TPA in EG (mol/kg)
α'	apparent solubility of TPA in reaction mixtures (mol/kg), defined as eq. (23)
θ	residence time of a reactor (min)
ρ	density of reaction mixtures (kg/L)
τ	characteristic dissolution time of solid TPA (min), defined as eq. (23)

REFERENCES

1. K. Ravindranath and R. A. Mashelkar, *Polym. Eng. Sci.*, **22**, 610 (1982).
2. T. Yamada and Y. Imamura, *Polym.-Plast. Technol. Eng.*, **28**, 811 (1989).
3. T. L. Mock, C.-C. Chen, D. L. Phipps, Jr., and R. A. Greenberg, in *AIChE Spring National Meeting*, 1988.
4. C.-K. Kang, B. C. Lee, and D. W. Ihm, *J. Appl. Polym. Sci.*, **60**, 2007 (1996).
5. ASPENPCD (Pure Component Data Bank of AspenPlus™), Aspen Technology, Inc.
6. T. Yamada, Y. Imamura, and O. Makimura, *Polym. Eng. Sci.*, **25**, 788 (1985).
7. H. K. Reimschuessel and B. T. Debona, *J. Polym. Sci. Polym. Chem. Ed.*, **17**, 3241 (1979).
8. J. Otton and S. Ratton, *J. Polym. Sci. Polym. Chem. Ed.*, **26**, 2183 (1988).
9. K. Ravindranath and R. A. Mashelkar, *J. Appl. Polym. Sci.*, **26**, 3179 (1981).
10. T. Yamada, Y. Imamura, and O. Makimura, *Polym. Eng. Sci.*, **26**, 708 (1986).
11. G.-D. Lei, PhD Thesis, University of Maryland, College Park, 1992.
12. G.-D. Lei and K. Y. Choi, *Ind. Eng. Chem. Res.*, **32**, 800 (1993).

Received April 1, 1996

Accepted July 16, 1996